Supporting Information

Bai et al. 10.1073/pnas.1203118109

SI Text

Friction Alone Cannot Explain Supercoil Relaxation Data. We briefly describe the bead velocity during supercoil relaxation [e.g., by topoisomerase (topo) IB] expected for a model with no thermal fluctuations. In this case the external (magnetic) force on the bead f_{ext} is balanced by velocity-dependent frictional forces. The bead is acted on by a drag force of $f_{bead} = 3\pi\eta D v$, where η is the solution viscosity, D is the effective bead diameter, and v is the bead velocity. The enzyme–DNA contact during relaxation also contributes a velocity-dependent force of the form $f_{enz} = \zeta_{enz} v$, where ζ_{enz} is a bead size-independent factor that takes into account the coupling of rotation to extension (each rotation releases 60 nm of DNA length) and the molecular friction. The terminal velocity v is determined by balancing these forces, or by $f_{ext} = f_{bead} + f_{enz}$, giving $v = f_{ext}/(3\pi\eta D + \zeta_{enz})$. Therefore, the inverse of the bead velocity would be:

$$\frac{1}{v} = \frac{3\pi\eta}{f_{ext}} D + \frac{\zeta_{enz}}{f_{ext}}.$$

In a friction-only model, the inverse of bead velocity should be linearly dependent on bead diameter D with an enzyme-independent slope and an enzyme-dependent intercept. Fig. S4 shows that the slope is dependent on enzyme, ruling out the friction-only model.

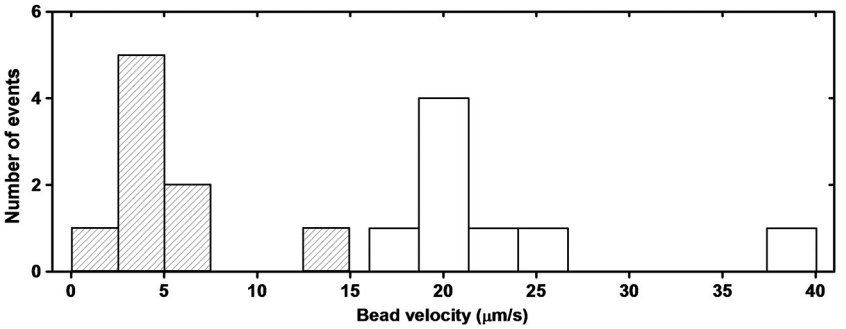

Fig. S1. Histograms of bead velocities found for relaxation of supercoils by topo IB, for 1 μm-diameter (white bars) and 2.8 μm-diameter (shaded bars) beads (0.5 pN, ΔLk = −30). The histograms show a peaked shape, with an approximately threefold shift in peak location.

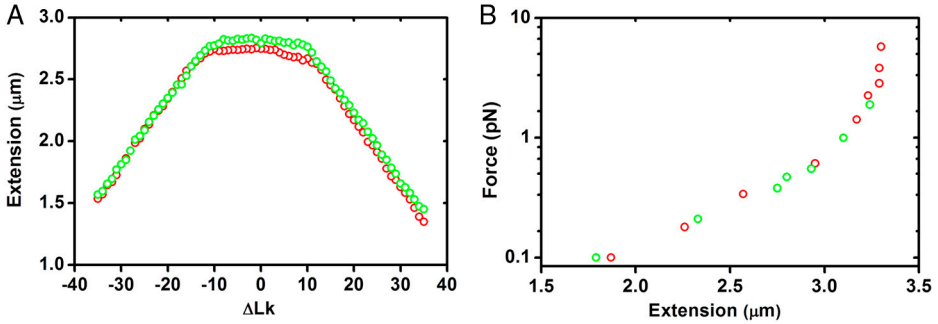

Fig. S2. Force calibration for 1-μm and 2.8-μm beads, for 0.5 pN. (*A*) Tether extension as a function of ΔLk, for stretching force 0.48 ± 0.02 pN. Green circles show data for a supercoilable DNA tethered to a 1-μm bead. The buckling points to enter the negative and positive plectonemic regimes are ΔLk = −13 and +11, respectively. Red circles show data for a 2.8-μm tethered bead, with buckling points at −14 and +12. Given that the hat curves are sensitive to the applied force, this result shows no observable error with our force calibrations for different bead sizes. (*B*) DNA extension as a function of applied force. Green circles and red circles show results for 1-μm and 2.8-μm tethered beads, respectively. The two curves coincide, showing no significant difference of force calibrations for different bead sizes.

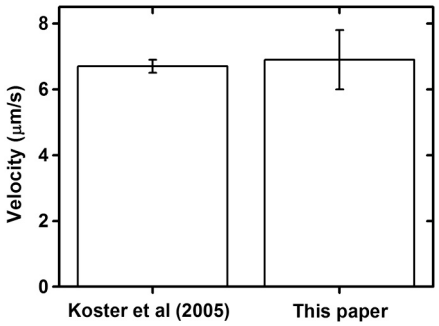

Fig. S3. Supercoil relaxation velocities for topo IB. (*Left*) Previous results (1) for 1-μm beads, 24-kb molecules, positive supercoiling, and a force of 0.2 pN; velocity was 6.7 ± 0.2 μm/s. (*Right*) Data of this paper using the same bead size and force for a 10-kb molecule; observed velocity was 6.9 ± 0.9 μm/s, in accord with the previous result. Although there is a twofold difference in total molecule length between the two experiments, the initial extension (approximately 1.3 μm) of the DNA in both experiments suggests that the initial spring constants for tension fluctuations were similar in the two experiments.

1 Koster DA, Croquette V, Dekker C, Shuman S, Dekker NH (2005) Friction and torque govern the relaxation of DNA supercoils by eukaryotic topoisomerase IB. *Nature* 434:671–674.

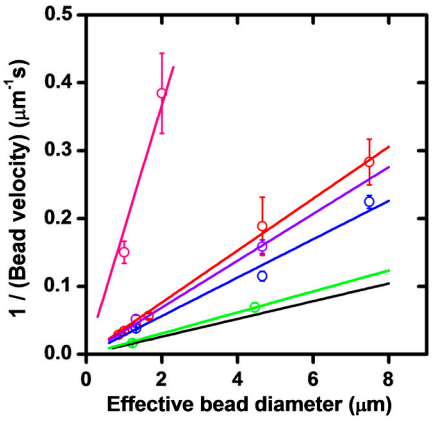

Fig. S4. Inverse bead velocity vs. effective bead diameter (0.5 pN, ΔLk = −30). The same data as in Fig. 3 are replotted; if bead drag coefficient were determining the relaxation velocity, one should see the same slopes for all curves. This plot rules out the possibility of a description using bead and enzyme friction without consideration of thermally crossed energy barriers at the enzyme–DNA interface.

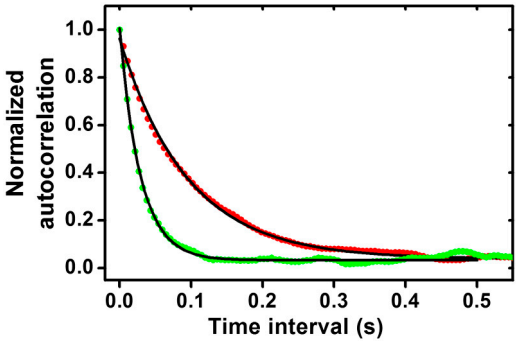

Fig. S5. Normalized autocorrelation functions of the thermal fluctuation for 1-μm (green) and 2.8-μm (red) tethered beads, under stretching force of 1.08 ± 0.02 pN. Solid black lines are fits to single-exponential decays. For the larger beads, the decay constant is 0.096 ± 0.012 s, and for smaller beads, the decay constant is 0.032 ± 0.002 s. The relaxation time of the beads is proportional to bead size within measurement error, indicating that the bead diffusion constant is controlling bead motion.

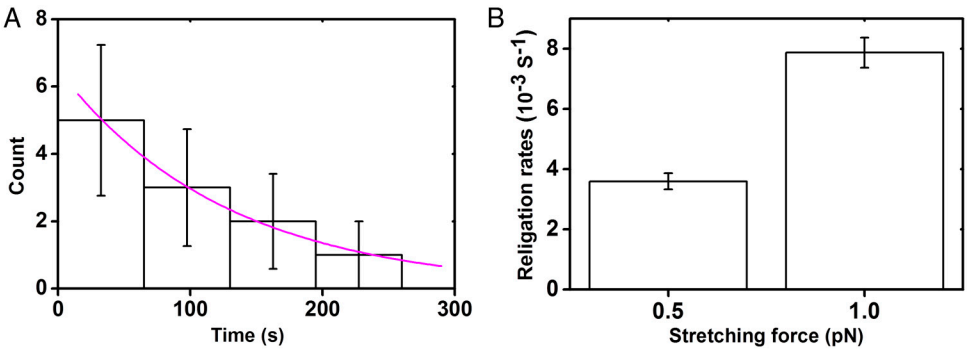

Fig. S6. Bxb1 integrase religation rate depends on applied force. Measurements of religation rate for Bxb1 integrase were carried out for constant forces of 0.5 ± 0.05 pN and 1.0 ± 0.05 pN on 2.8 μm-diameter magnetic beads following observation of supercoil relaxation. (*A*) A series of waiting times between relaxation and religation events under stretching force of 1.0 ± 0.05 pN was measured and histogrammed. The resulting distribution was fit with a first-order exponential decay. Religation rate was calculated from the decay constant. (*B*) For 0.5 pN, the religation rate was $3.6 \pm 0.3 \bullet 10^{-3}$ s^{-1} (data from Fig. 4), whereas for 1.0 pN, the rate was $7.9 \pm 0.5 \bullet 10^{-3}$ s^{-1}, approximately twofold faster.

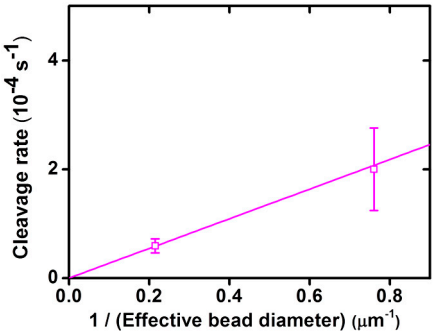

Fig. S7. Reaction rates for DNA cleavage in Bxb1 integrase supercoil relaxation experiments, for 2.8 μm-diameter beads and 1 μm-diameter beads. Time to DNA cleavage following addition of Bxb1 recombinase and recombining DNA oligo was measured. Reaction rates were calculated using the total number of relaxation events per total reaction time, for force of 0.5 pN and initial ΔLk of −30. Dependence of the rates on the inverse of effective bead diameters was observed. We note that the complex nature of this reaction, which involves diffusive search for target and formation of an active tetrameric enzyme complex before binding and cleavage can occur, makes this a somewhat less convincing demonstration of the effect than the essentially unimolecular religation reaction (Fig. 4).

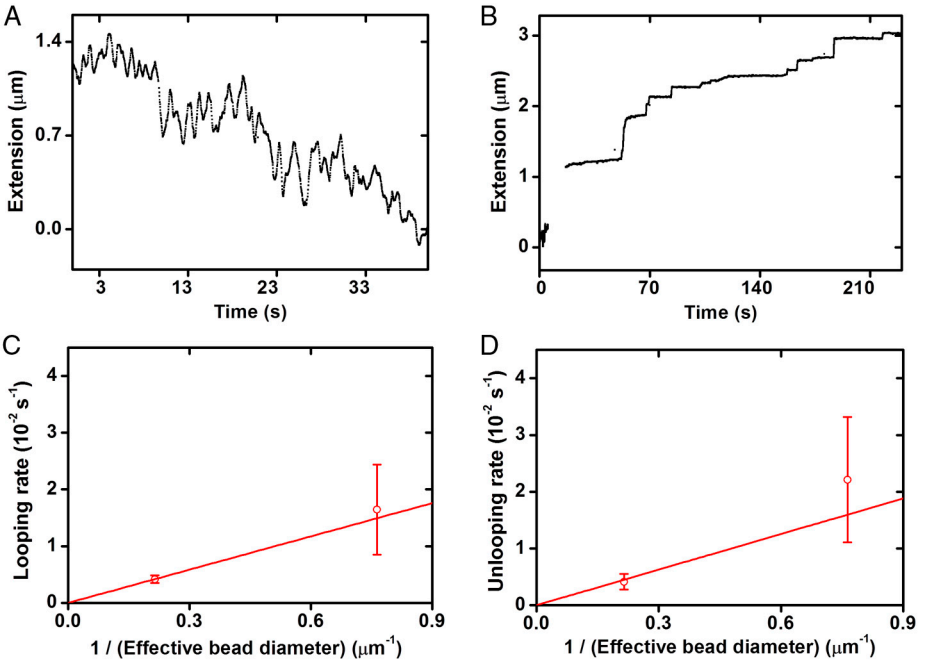

Fig. S8. Dependence of reaction rates for Fis-generated nonspecific looping and unlooping on the inverse of effective bead diameter. Fis is an abundant DNA-binding protein in *Escherichia coli* during rapid growth, and one of its functions is to help establish nucleoid structure. Nonspecific binding of Fis causes DNA to compact (at nanomolar concentration levels) and loop (above 1 μM concentration) (1). In single-molecule experiments, the opening and closing of loops on single DNA molecules can be followed in real time as jumps in DNA extension, allowing measurement of the reaction rates (1). Looping occurs at low forces (approximately 0.1 pN); following folding of a DNA, unlooping can be driven by larger forces (approximately 3 pN). (*A*) Real-time trace of an example looping

reaction for Fis-coated DNA with 2.8-μm bead. DNA underwent complete looping condensation in 223 s (the time between setting stretching force to 0.1 pN and full collapse; figure only shows the end of this process). (*B*) Example trace of an unlooping event with 2.8-μm bead. The waiting time between setting force to 3 pN and DNA returning to full extension was 199 s. (*C*) Looping rates for 1 μm-diameter and 2.8 μm-diameter beads. (*D*) Unlooping rates for 1 μm-diameter and 2.8 μm-diameter beads. Both looping and unlooping rates are approximately proportional to the inverse of effective bead diameters.

1 Skoko D, et al. (2006) Mechanism of chromosome compaction and looping by the *Escherichia coli* nucleoid protein Fis. *J Mol Biol* 364:777–798.

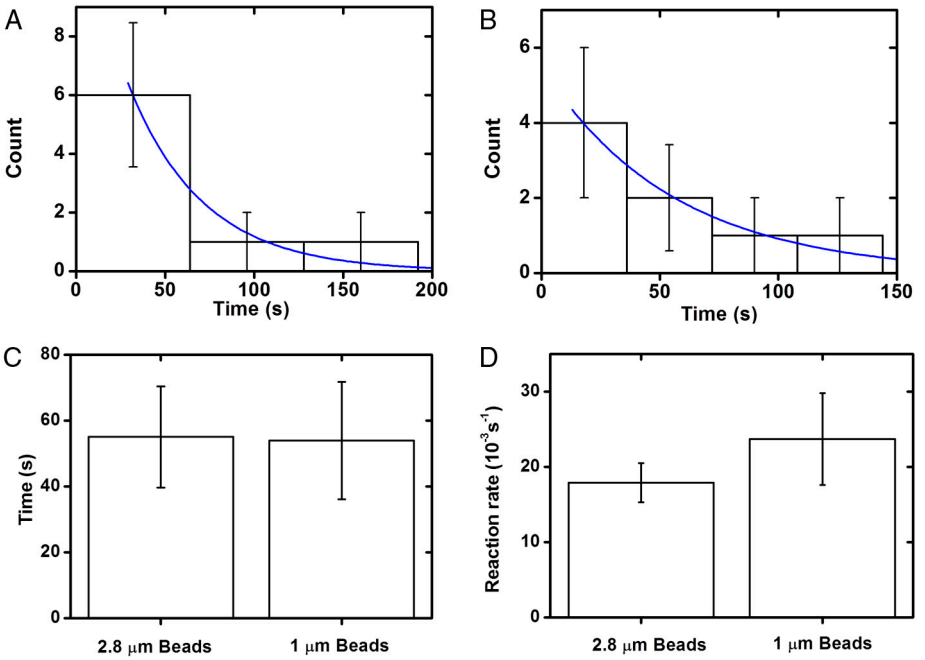

Fig. S9. Reaction times for PvuII DNA-cutting experiments (0.5 pN) do not show a bead-size dependence. Enzyme in buffer (0.06 units/μL) was introduced, and the time at which DNA cleavage was observed was recorded. (*A*) Distribution of waiting times to cleavage for 1-μm bead showing fit to exponential. (*B*) Distribution of waiting times to cleavage for 2.8-μm bead. (*C*) Average waiting times to cleavage, following flow through of enzyme solution. (*Left*) Average waiting time for 2.8 μm-diameter bead release was 55 ± 15 s. (*Right*) Average waiting time for 1 μm-diameter bead release was 54 ± 18 s. Time to bead release shows no statistically significant dependence on bead size. (*D*) Time to cleavage determined from exponential fits of *A*; results are in good accord with *C*.

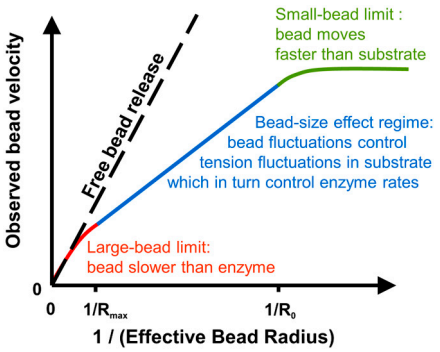

Fig. S10. Sketch of expected small- and large-bead limits on observed bead velocity in DNA supercoil relaxation experiments of the type shown in Fig. 3. For very small beads (green, $R < R_0$) bead motion will be fast enough not to limit tension fluctuations inside the DNA, and the relaxation velocity will be observed to approach a constant dependent on the dynamics of the DNA substrate itself. This can be expected to occur for beads comparable in size to the conformational size of the DNA. For very large beads (red, $R > R_{max}$), bead motion will become so slow that enzyme activity will occur quickly compared to bead motion, so bead velocity equal to the free bead release velocity will be observed. Experiments of this paper are in the intermediate regime (blue) where bead motion is slow enough to limit the rate at which tension fluctuates in the molecule, but not so slow that those fluctuations occur on timescales much longer than the enzyme-catalyzed reaction.

Table S1. Effective diameters for beads used in the release experiments and supercoil relaxation experiments

Actual bead diameter(μm)	Enhancement coefficient	Effective bead diameter(μm)	Release limit(μm/s)
	Bead release experiments*		
3.96†	1.81	7.15	10.72
2.80	1.59	4.46	17.18
1.20	1.26	1.51	50.59
1.00	1.22	1.22	62.88
0.80	1.18	0.95	81.04
0.70	1.16	0.81	94.44
	Supercoil relaxation experiments‡		
3.96†	1.89	7.48	
2.80	1.66	4.66	
1.20	1.38	1.65	
1.00	1.31	1.31	
0.80	1.25	1.00	
0.70	1.22	0.85	

The drag coefficient for a sphere close to a plane surface is a function of the actual diameter of this sphere and the distance to the plane (1). In the bead release experiments and the supercoil relaxation experiments, this distance varies (i.e., the starting points of beads are different). One can include this enhancement effect into the bead sizes, to calculate the effective bead diameters for particular experiments.

*In bead release experiments, beads were held approximately 2.5 μm away from the surface before cleavage. The theoretical expectation values for release velocities are also shown.

†Indicates effective diameter for double 2.8 μm-diameter bead (two 2.8-μm beads stuck together). This double-bead structure is treated as an ellipsoid; its drag coefficient is estimated and used to obtain an estimate of the equivalent effective bead diameter through the Stokes drag formula for a sphere.

‡For supercoil relaxation experiments for 0.5-pN force, beads were initially approximately 1.8 μm from surface (Fig. 2), a smaller distance than that for bead release experiments*, leading to a larger drag enhancement.

1 Brenner H (1961) The slow motion of a sphere through a viscous fluid towards a plane surface. *Chem Eng Sci* 16:242–251.